References

Acik, M., Lee, G., Mattevi, C., Pirkle, A., Wallace, R.M., Chhowalla, M., Cho, K., Chabal, Y., 2011. The role of oxygen during thermal reduction of graphene oxide studied by infrared absorption spectroscopy. J. Phys. Chem. C 115, 19761–19781.

Adhvaryu, A., Erhan, S.Z., Perez, J.M., 2004. Preparation of Soybean Oil-Based Greases : Effect of Composition and Structure on Physical Properties. J. Agric. Food Chem. 52, 6456–6459.

Adhvaryu, A., Sung, C., Erhan, S.Z., 2005. Fatty acids and antioxidant effects on grease microstructures. Ind. Crops Prod. 21, 285–291.

Akhtar, K., Khalid, H., Haq, I.U., Malik, A., 2016. Improvement in tribological properties of lubricating grease with quartz-enriched rice husk ash. Tribiology Int. 93, 58–62.

Asrul, M., Zulkifli, N.W.M., Masjuki, H.H., Kalam, M.A., 2013. Tribological properties and lubricant mechanism of nanoparticle in engine oil. Procedia Eng. 68, 320–325.

ASTM-D1403, 2010. Standard Test Methods for Cone Penetration of Lubricating Grease Using One-Quarter and One-Half Scale Cone Equipment. ASTM Int.

ASTM-D217, 2003. Standard Test Methods for Cone Penetration of Lubricating Grease. ASTM Int.

ASTM-D2265, 2015. Standard Test Method for Dropping Point of Lubricating Grease Over Wide Temperature Range. ASTM Int.

ASTM-D2266, 2002. Standard Test Method for Wear Preventive Characteristics of Lubricating Grease (Four-Ball Method). ASTM Int.

ASTM-D2596, 2015. Standard Test Method for Measurement of Extreme-Pressure Properties of Lubricating Grease (Four-Ball Method). ASTM Int.

ASTM-D566, 2016. Standard Test Method for Dropping Point of Lubricating Grease. ASTM Int.

ASTM-D5707-16, 2017. Standard Test Method for Measuring Friction and Wear

Properties of Lubricating Grease Using a High-Frequency, Linear-Oscillation (SRV) Test machine. ASTM Int.

Azman, S.S.N., Zulkifli, N.W.M., Masjuki, H., Gulzar, M., Zahid, R., 2016. Study of tribological properties of lubricating oil blend added with graphene nanoplatelets. J. Mater. Res. 31, 1932–1938.

Barriga, J., Igartua, A., Aranzabe, A., 2005. Sunflower based grease for heavy duty applications, in: World Tribology Congress III. ASME, Washington, D.C., pp. 481–482.

Battez, A.H., González, R., Viesca, J.L., Fernández, J.E., Fernández, J.D., Machado, A., Chou, R., Riba, J., 2008. CuO, ZrO_2 and ZnO nanoparticles as antiwear additive in oil lubricants. Wear 265, 422–428.

Berman, D., Erdemir, A., Zinovev, A. V, Sumant, A. V, 2015. Nanoscale friction properties of graphene and graphene oxide. Diam. Relat. Mater. 54, 91–96.

Bhaumik, S., Kamaraj, M., Paleu, V., 2021. Tribological analyses of a new optimized gearbox biodegradable lubricant blended with reduced graphene oxide nanoparticles. Proc. Inst. Mech. Eng. Part J J. Eng. Tribol. 235, 901–915.

Boshui, C., Kecheng, G., Jianhua, F., Jiang, W., Jiu, W., Nan, Z., 2015. Tribological characteristics of monodispersed cerium borate nanospheres in biodegradable rapeseed oil lubricant. Appl. Surf. Sci. 353, 326–332.

Buczek, B., Zajezierska, A., 2015. Biodegradable lubricating greases containing used frying oil as additives. Ind. Lubr. Tribol. 67, 315–319.

Cann, P.M., 2007. Grease lubrication of rolling element bearings — role of the grease thickener. Lubr. Sci. 19, 183–196.

Chang, H., Kao, M., Luo, J., Lan, C., 2015. Synthesis and Effect of Nanogrease on Tribological Properties. Int. J. Precis. Eng. Manuf. 16, 1311–1316.

Chang, H., Lan, C.W., Chen, C.H., Kao, M.J., Guo, J. Bin, 2014. Anti-wear and friction properties of nanoparticles as additives in the lithium grease. Int. J. Precis. Eng. Manuf. 15, 2059–2063.

Chen, J., 2010. Tribological properties of polytetrafluoroethylene, nano-titanium dioxide, and nano-silicon dioxide as additives in mixed oil-based titanium complex grease. Tribol. Lett. 38, 217–224.

Chen, T., Xia, Y., Liu, Z., Wang, Z., 2014. Preparation and tribological properties of attapulgite – bentonite clay base grease. Ind. Lubr. Tribol. 66, 538–544.

Cheng, Z.L., Qin, X.X., 2014. Study on friction performance of graphene-based semi-solid grease. Chinese Chem. Lett. 25, 1305–1307.

Choi, W., Lee, J. (Eds.), 2012. Graphene synthesis and applications. CRC press, Taylor & Francis Group, Boca Raton.

Choudhary, S., Mungse, H.P., Khatri, O.P., 2012. Dispersion of alkylated graphene in organic solvents and its potential for lubrication applications. J. Mater. Chem. 22, 21032–21039.

Chouhan, A., Mungse, H.P., Khatri, O.P., 2020a. Surface chemistry of graphene and graphene oxide : A versatile route for their dispersion and tribological applications. Adv. Colloid Interface Sci. 283, 102215.

Chouhan, A., Mungse, H.P., Sharma, O.P., Singh, R.K., Khatri, O.P., 2018. Chemically functionalized graphene for lubricant applications: Microscopic and spectroscopic studies of contact interfaces to probe the role of graphene for enhanced tribo-performance. J. Colloid Interface Sci. 513, 666–676.

Chouhan, A., Sarkar, T.K., Kumari, S., Vemuluri, S., Khatri, O.P., 2020b. Synergistic lubrication performance by incommensurately stacked ZnO- decorated reduced graphene oxide/MoS_2 heterostructure. J. Colloid Interface Sci. 580, 730–739.

Cizaire, L., Vacher, B., Le Mogne, T., Martin, J.M., Rapoport, L., Margolin, A., Tenne, R., 2002. Mechanisms of ultra-low friction by hollow inorganic fullerene-like MoS_2 nanoparticles. Surf. Coatings Technol. 160, 282–287.

Couronne, I., Vergne, P., 2000. Rheological Behavior of Greases: Part II — Effect of Thermal Aging, Correlation with Physico-Chemical Changes. Tribol. Trans. 43, 788–794.

Couronné, I., Vergne, P., Mazuyer, D., Truong-Dinh, N., Girodin, D., 2003. Effects of Grease Composition and Structure on Film Thickness in Rolling Contact. Tribol. Trans. 46, 31–36.

Dai, W., Kheireddin, B., Gao, H., Liang, H., 2016. Roles of nanoparticles in oil lubrication. Tribiology Int. 102, 88–98.

Dai, Y., Niu, W., Zhang, X., Xu, H., Dong, J., 2017. Tribological Investigation of Layered Zirconium Phosphate in Anhydrous Calcium Grease. Lubricants 5, 22–31.

Delgado, M.A., Sánchez, M.C., Valencia, C., Franco, J.M., Gallegos, C., 2005. Relationship among microstructure, rheology and processing of a lithium lubricating grease. Chem. Eng. Res. Des. 83, 1085–1092.

Ehrlich, M. (Ed.), 1984. NLGI lubricating grease guide, First. ed. NLGI, Missouri, USA.

Fan, X., Li, W., Li, H., Zhu, M., Xia, Y., Wang, J., 2018. Probing the effect of thickener on tribological properties of lubricating greases. Tribol. Int. 118, 128–139.

Fan, X., Xia, Y., Wang, L., Li, W., 2014. Multilayer graphene as a lubricating additive in bentone grease. Tribol. Lett. 55, 455–464.

Fiedler, M., Kuhn, E., Franco, J.M., Litters, T., 2011. Tribological Properties of Greases Based on Biogenic Base Oils and Traditional Thickeners in Sapphire-Steel Contact. Tribol. Lett. 44, 293–304.

Finnie, K.S., Cassidy, D.J., Bartlett, J.R., Woolfrey, J.L., 2001. IR spectroscopy of surface water and hydroxyl species on nanocrystalline TiO_2 films. Langmuir 17, 816–820.

Florea, O., Luca, M., Constantinescu, A., Florescu, D., 2003. The Influence of Lubricating Fluid Type on the Properties of Biodegradable Greases. J. Synth. Lubr. 19, 303–313.

Fox, N.J., Stachowiak, G.W., 2007. Vegetable oil-based lubricants-A review of oxidation. Tribol. Int. 40, 1035–1046.

Gadelmawla, E.S., Koura, M.M., Maksoud, T.M.A., Elewa, I.M., Soliman, H.H., 2002. Roughness parameters. J. Mater. Process. Technol. 123, 133–145.

Gallego, R., Cidade, T., Sánchez, R., Valencia, C., Franco, J.M., 2016. Tribological

behaviour of novel chemically modified biopolymer-thickened lubricating greases investigated in a steel – steel rotating ball-on-three plates tribology cell. Tribiology Int. 94, 652–660.

Gan, C., Liang, T., Chen, D., Li, W., Fan, X., Tang, G., Lin, B., Zhu, M., 2020. Phosphonium-organophosphate modified graphene gel towards lubrication applications. Tribol. Int. 145, 106180.

Gan, X., Lv, R., Wang, X., Zhang, Z., Fujisawa, K., Lei, Y., Huang, Z., Terrones, M., Kang, F., 2018. Pyrolytic carbon supported alloying metal dichalcogenides as free-standing electrodes for efficient hydrogen evolution. Carbon N. Y. 132, 512–519.

Gänsheimer, J., Holinski, R., 1972. A study of solid lubricants in oils and greases under boundary conditions. Wear 19, 439–449.

García-Zapateiro, L.A., Valencia, C., Franco, J.M., 2014. Formulation of lubricating greases from renewable basestocks and thickener agents: A rheological approach. Ind. Crops Prod. 54, 115–121.

Ge, X., Xia, Y., Cao, Z., 2015. Tribological properties and insulation effect of nanometer TiO_2 and nanometer SiO_2 as additives in grease. Tribol. Int. 92, 454–461.

Ge, X., Xia, Y., Feng, X., 2016. Influence of Carbon Nanotubes on Conductive Capacity and Tribological Characteristics of Poly(ethylene Glycol-Ran-Propylene Glycol) Monobutyl Ether as Base Oil of Grease. J. Tribol. 138, 11801.

Georgakilas, V., Tiwari, J.N., Kemp, K.C., Perman, J.A., Bourlinos, A.B., Kim, K.S., Zboril, R., 2016. Noncovalent Functionalization of Graphene and Graphene Oxide for Energy Materials, Biosensing, Catalytic, and Biomedical Applications. Chem. Rev. 116, 5464–5519.

Gerpen, J. Van, 2005. Biodiesel processing and production. Fuel Process. Technol. 86, 1097–1107.

Ghaednia, H., Jackson, R.L., Khodadadi, J.M., 2016. Experimental analysis of stable CuO nanoparticle enhanced lubricants. J. Exp. Nanosci. 10, 1–18.

Gonçalves, D., Vieira, A., Carneiro, A., Campos, A. V., Seabra, J.H.O., 2017. Film

Thickness and Friction Relationship in Grease Lubricated Rough Contacts. Lubricants 5, 34.

Guimarey, M.J., Abdelkader, A.M., Comuñas, M.J., Alvarez-Lorenzo, C., Thomas, B., Fernández, J., Hadfield, M., 2020. Comparison between thermophysical and tribological properties of two engine lubricant additives : electrochemically exfoliated graphene and molybdenum disulfide nanoplatelets. Nanotechnology 32, 25701.

Gulzar, M., Masjuki, H.H., Kalam, M.A., Varman, M., Zulkifli, N.W.M., Mufti, R.A., Zahid, R., 2016. Tribological performance of nanoparticles as lubricating oil additives. J. Nanoparticle Res. 18, 223.

Gulzar, M., Masjuki, H.H., Varman, M., Kalam, M.A., Mufti, R.A., Zulki, N.W.M., Yunus, R., Zahid, R., 2015. Improving the AW/EP ability of chemically modified palm oil by adding CuO and MoS_2 nanoparticles. Tribol. Int. 88, 271–279.

Gupta, R.N., Harsha, A.P., 2018a. Antiwear and extreme pressure performance of castor oil with nano-additives. Proc. Inst. Mech. Eng. Part J J. Eng. Tribol. 232, 1055–1067.

Gupta, R.N., Harsha, A.P., 2018b. Tribological evaluation of calcium-copper-titanate/cerium oxide-based nanolubricants in sliding contact. Lubr. Sci. 30, 175–187.

Gupta, R.N., Harsha, A.P., 2017. Synthesis, characterization, and Tribological studies of calcium-copper-Titanate Nanoparticles as a Biolubricant additive. J. Tribol. 139, 21801.

Gupta, R.N., Harsha, A.P., Singh, S., 2018. Tribological study on rapeseed oil with nano-additives in close contact sliding situation. Appl. Nanosci. 8, 567–580.

He, Q., Li, A., Guo, Y., Liu, S., Zhang, Y., Kong, L., 2018. Tribological properties of nanometer cerium oxide as additives in lithium grease. J. Rare Earths 36, 209–214.

Holmberg, K., Andersson, P., Erdemir, A., 2012. Global energy consumption due to friction in passenger cars. Tribiology Int. 47, 221–234.

Holmberg, K., Andersson, P., Nylund, N., Mäkelä, K., Erdemir, A., 2014. Global energy consumption due to friction in trucks and buses. Tribiology Int. 78, 94–114.

Holmberg, K., Siilasto, R., Laitinen, T., Andersson, P., Ari, J., 2013. Global energy consumption due to friction in paper machines. Tribol. Int. 62, 58–77.

Honary, L.A.T., Richter, E., 2011. Biobased lubricants and greases: Technology and products, First. ed. John Wiley & Sons, Ltd., Chichester.

Hongtao, L., Hongmin, J., Haiping, H., Younes, H., 2014. Tribological properties of carbon nanotube grease. Ind. Lubr. Tribol. 66, 579–583.

Hu, E.Z., Xu, Y., Hu, K.H., Hu, X.G., 2017. Tribological properties of 3 types of MoS_2 additives in different base greases. Lubr. Sci. 29, 541–555.

Hu, H.K., Hu, X.G., Xu, Y.F., Huang, F., Liu, J.S., 2010. The Effect of Morphology on the Tribological Properties of MoS_2 in Liquid Paraffin. Tribol. Lett. 40, 155–165.

Hutchings, I., Shipway, P., 2017. Tribology Friction and Wear of Engineering Materials, Second. ed. Butterworth-Heinemann., Oxford, United Kingdom.

Ishchuk, Y.L., 2005. Lubricating Grease Manufacturing Technology. New Age International (P) Limited, New Delhi, India.

Jafarzadeh, M., Rahman, I.A., Sipaut, C.S., 2009. Synthesis of silica nanoparticles by modified sol-gel process: The effect of mixing modes of the reactants and drying techniques. J. Sol-Gel Sci. Technol. 50, 328–336.

Jayadas, N.H., Nair, K.P., 2006. Coconut oil as base oil for industrial lubricants — evaluation and modification of thermal, oxidative and low temperature properties. Tribiology Int. 39, 873–878.

Jayadas, N.H., Prabhakaran Nair, K., G, A., 2007. Tribological evaluation of coconut oil as an environment-friendly lubricant. Tribol. Int. 40, 350–354.

Ji, X., Chen, Y., Zhao, G., Wang, X., Liu, W., 2011. Tribological properties of $CaCO_3$ nanoparticles as an additive in lithium grease. Tribol. Lett. 41, 113–119.

Jing, W., Xiaochuan, G., Yan, H., Mingjun, J., Wanqing, G., Youantao, Z., Rong, S., 2017. Tribological Characteristics of Graphene as Lithium Grease Additive. China Pet. Process. Petrochemical Technol. 19, 46–54.

Kamel, B.M., Mohamed, A., El-Sherbiny, M., Abed, K.A., Abd-Rabou, M., 2017. Rheological characteristics of modified calcium grease with graphene nanosheets. Fullerenes Nanotub. Carbon Nanostructures 25, 429–434.

Kamel, B.M., Mohamed, A., El Sherbiny, M., Abed, K.A., 2016. Tribological behaviour of calcium grease containing carbon nanotubes additives. Ind. Lubr. Tribol. 68, 723–728.

Kamel, B.M., Mohamed, A., Sherbiny, M. El, Abed, K.A., Kamel, B.M., Mohamed, A., Sherbiny, M. El, Abed, K.A., 2017. Tribological properties of graphene nanosheets as an additive in calcium grease. J. Dispers. Sci. Technol. 38, 1495–1500.

Kashyap, A., Harsha, A.P., 2016. Tribological studies on chemically modified rapeseed oil with CuO and CeO_2 nanoparticles. Proc. Inst. Mech. Eng. Part J J. Eng. Tribol. 230, 1562–1571.

Kobayashi, K., Hironaka, S., Tanaka, A., Umeda, K., Iijima, S., Yudasaka, M., Kasuya, D., Suzuki, M., 2005. Additive Effect of Carbon Nanohorn on Grease Lubrication Properties. J. Japan Pet. Inst. 48, 121–126.

Koshy, C.P., Rajendrakumar, K.P., Thottackkad, M.V., 2015. Evaluation of the tribological and thermo-physical properties of coconut oil added with MoS_2 nanoparticles at elevated temperatures. Wear 331, 288–308.

Kumar, H., Harsha, A.P., 2020. Investigation on Friction, Anti- wear, and Extreme Pressure Properties of Different Grades of Polyalphaolefins With Functionalized Multi-walled Carbon Nanotubes as an Additive. J. Tribol. 142, 81702.

Kumari, S., Gusain, R., Kumar, N., Khatri, O.P., 2016. PEG-mediated hydrothermal synthesis of hierarchical microspheres of MoS_2 nanosheets and their potential for lubrication application. J. Ind. Eng. Chem. 42, 87–94.

Kumari, S., Mungse, H.P., Gusain, R., Kumar, N., Sugimura, H., Khatri, O.P., 2017. Octadecanethiol-grafted molybdenum disulfide nanosheets as oil-dispersible additive for reduction of friction and wear. FlatChem 3, 16–25.

Lansdown, A.R., 2004. Lubrication and Lubricant Selection: A practical Guide, Thrid. ed.

Professional Engineering Publishing Limited, London.

Liang, T., Sawyer, W.G., Perry, S.S., Sinnott, S.B., Phillpot, S.R., 2011. Energetics of oxidation in MoS_2 nanoparticles by density functional theory. J. Phys. Chem. C 115, 10606–16.

Liu, D., Zhao, G., Wang, X., 2012. Tribological performance of lubricating greases based on calcium carbonate polymorphs under the boundary lubrication condition. Tribol. Lett. 47, 183–194.

Lugt, P.M., 2013. Grease Lubrication in Rolling Bearings. John Wiley & Sons, Ltd, Chichester, United Kingdom.

Lugt, P.M., 2009. A Review on Grease Lubrication in Rolling Bearings. Tribol. Trans. 52, 470–480.

Mang, T., Dresel, W. (Eds.), 2007. Lubricants and Lubrication, Second. ed. WILEY-VCH Verlag GmbH & Co. KGaA, Weinheim.

Mannekote, J.K., Kailas, S. V, 2009. Studies on boundary lubrication properties of oxidised coconut and soy bean oils. Lubr. Sci. 21, 355–365.

Martín-Alfonso, J.E., Núñez, N., Valencia, C., Franco, J.M., Diaz, M.J., 2011. Formulation of new biodegradable lubricating greases using ethylated cellulose pulp as thickener agent. J. Ind. Eng. Chem. 17, 818–823.

Menezes, P.L., Ingole, S.P., Nosonovsky, M., Kailas, S. V., Lovell, M.R. (Eds.), 2013. Tribology for Scientists and Engineers. Springer, New York.

Mobarak, H.M., Mohamad, E.N., Masjuki, H.H., Kalam, M.A., Mahmud, K.A.H. Al, Habibullah, M., Ashraful, A.M., 2014. The prospects of biolubricants as alternatives in automotive applications. Renew. Sustain. Energy Rev. 33, 34–43.

Mohamed, A., Osman, T.A., Khattab, A., Zaki, M., 2015. Tribological Behavior of Carbon Nanotubes as an Additive on Lithium Grease. J. Tribol. 137, 11801.

Mungse, H.P., Khatri, O.P., 2014. Chemically functionalized reduced graphene oxide as a novel material for reduction of friction and wear. J. Phys. Chem. C 118, 14394–14402.

Mungse, H.P., Singh, R., Sugimura, H., Kumar, N., Khatri, O.P., 2015. Molecular pillar supported graphene oxide framework: conformational heterogeneity and tunable d-spacing. Phys. Chem. Chem. Phys. 17, 20822–20829.

Nagaraju, G., Tharamani, C.N., Chandrappa, G.T., Livage, J., 2007. Hydrothermal synthesis of amorphous MoS_2 nanofiber bundles via acidification of ammonium heptamolybdate tetrahydrate. Nanoscale Res. Lett. 2, 461–468.

Nagendramma, P., Kaul, S., 2012. Development of ecofriendly/biodegradable lubricants: An overview. Renew. Sustain. Energy Rev. 16, 764–774.

Nagendramma, P., Kumar, P., 2015. Eco-Friendly Multipurpose Lubricating Greases from Vegetable Residual Oils. Lubricants 3, 628–636.

Ni, J., Feng, G., Meng, Z., Hong, T., Chen, Y., Zheng, X., 2018. Reinforced lubrication of vegetable oils with graphene additive in tapping ADC12 aluminum alloy. Int. J. Adv. Manuf. Technol. 94, 1031–1040.

Niu, M., Qu, J., 2018. Tribological properties of nano-graphite as an additive in mixed oil-based titanium complex grease. RSC Adv. 8, 42133–42144.

Nosonovsky, M., Bhushan, B. (Eds.), 2012. Green Tribology: Biomimetics, Energy Conservation and Sustainability. Springer Science & Business Media, Heidelberg.

Ogunniyi, D.S., 2006. Castor oil: A vital industrial raw material. Bioresour. Technol. 97, 1086–1091.

Onodera, T., Morita, Y., Suzuki, A., Koyama, M., Tsuboi, H., Minfray, C., Joly-pottuz, L., Martin, J., Miyamoto, A., 2009. A Computational Chemistry Study on Friction of h-MoS_2. Part I. Mechanism of Single Sheet Lubrication. J. Phys. Chem. B 113, 16526–16536.

OPEC-Report, 2019. Organization of the Petroleum Exporting Countries World Oil Outlook.

Padgurskas, J., Rukuiža, R., Kupcinskas, A., Kreivaitis, R., 2015. Lubrication properties of modified lard and rapeseed oil greases with sodium and lithium thickeners. Ind. Lubr. Tribol. 67, 557–563.

Panchal, T., Chauhan, D., Thomas, M., Patel, J., 2015. Bio based grease A value added product from renewable resources. Ind. Crops Prod. 63, 48–52.

Panchal, T.M., Patel, A., Chauhan, D.D., Thomas, M., Patel, J. V, 2017. A methodological review on bio-lubricants from vegetable oil based resources. Renew. Sustain. Energy Rev. 70, 65–70.

Paul, G., Shit, S., Hirani, H., Kuila, T., Murmu, N.C., 2019. Tribological behavior of dodecylamine functionalized graphene nanosheets dispersed engine oil nanolubricants. Tribol. Int. 131, 605–619.

Peña-Parás, L., Taha-Tijerina, J., García, A., Maldonado, D., Nájera, A., Cantú, P., Ortiz, D., 2015. Thermal transport and tribological properties of nanogreases for metal-mechanic applications. Wear 332–333, 1322–1326.

Polishuk, A.T., 1971. Mixed complex aluminum soap-clay grease composition. U.S. Patent 3,620,975.

Prabhu, K.N., Fernades, P., Kumar, G., 2009. Effect of substrate surface roughness on wetting behaviour of vegetable oils. Mater. Des. 30, 297–305.

Qiang, H., Anling, L., Yangming, Z., Liu, S., Yachen, G., 2017. Experimental study of tribological properties of lithium-based grease with Cu nanoparticle additive. Tribol. -Mater. Surfaces Interfaces 11, 75–82.

Rahman, I.A., Vejayakumaran, P., Sipaut, C.S., Ismail, J., Bakar, M.A., Adnan, R., Chee, C.K., 2007. An optimized sol–gel synthesis of stable primary equivalent silica particles. Colloids Surfaces A Physicochem. Eng. Asp. 294, 102–110.

Rastogi, R.B., Maurya, J.L., Jaiswal, V., Maurya, J.L., Saps, V.J.Z., 2013. Zero SAPs and Ash Free Antiwear Additives : Schiff Bases of Salicylaldehyde with 1,2-Phenylenediamine, 1,4-Phenylenediamine, and 4,4′-Diaminodiphenylenemethane and Their Synergistic Interactions with Borate Ester. Tribol. Trans. 56, 592–606.

Rizvi, S.Q.A., 2009. A Comprehensive Review of Lubricant Chemistry , Technology , Selection , and Design. ASTM International, West Conshohocken, PA.

Rudnick, L.R. (Ed.), 2017. Lubricant Additives: Chemistry and Applications, Third. ed.

CRC press, Taylor & Francis Group, Boca Raton.

Rudnick, L.R. (Ed.), 2006. Synthetics, Mineral Oils, and Bio-Based Lubricants Chemistry and Technology. CRC press, Taylor & Francis Group, Boca Raton.

Sahoo, R.R., Biswas, S.K., 2014. Effect of layered MoS_2 nanoparticles on the frictional behavior and microstructure of lubricating greases. Tribol. Lett. 53, 157–171.

Sahoo, R.R., Biswas, S.K., 2009. Frictional response of fatty acids on steel. J. Colloid Interface Sci. 333, 707–718.

Sajeeb, A., Rajendrakumar, P.K., 2020. Tribological assessment of vegetable oil based CeO_2/CuO hybrid nano-lubricant. Proc. Inst. Mech. Eng. Part J J. Eng. Tribol. 234, 1940–1956.

Salomonsson, L., Stang, G., Zhmud, B., 2008. Oil/Thickener Interactions and Rheology of Lubricating Greases. Tribol. Trans. 50, 302–309.

Sánchez, R., Franco, J.M., Delgado, M.A., Valencia, C., Gallegos, C., 2011. Thermal and mechanical characterization of cellulosic derivatives-based oleogels potentially applicable as bio-lubricating greases: Influence of ethyl cellulose molecular weight. Carbohydr. Polym. 83, 151–158.

Sánchez, R., Franco, J.M., Delgado, M.A., Valencia, C., Gallegos, C., 2009. Development of new green lubricating grease formulations based on cellulosic derivatives and castor oil. Green Chem. 11, 686–693.

Schultheiss, H., Tobie, T., Stahl, K., 2016. The Effect of Selected Grease Components on the Wear Behavior of Grease-Lubricated Gears. J. Tribol. 138, 11602.

Shafi, W.K., Charoo, M.S., 2021. An overall review on the tribological, thermal and rheological properties of nanolubricants. Tribol. - Mater. Surfaces Interfaces 15, 20–54.

Shariq, B., Charoo, M.S., 2019. Effect of Additives on the Tribological Properties of Various Greases-A Review. Mater. Today Proc. 18, 4416–4420.

Sharma, B.K., Adhvaryu, A., Perez, J.M., Erhan, S.Z., 2006. Biobased grease with

improved oxidation performance for industrial application. J. Agric. Food Chem. 54, 7594–7599.

Sharma, B.K., Adhvaryu, A., Perez, J.M., Erhan, S.Z., 2005. Soybean oil based greases: Influence of composition on thermo-oxidative and tribochemical behavior. J. Agric. Food Chem. 53, 2961–2968.

Shen, T., Wang, D., Yun, J., Liu, Q., Liu, X., Peng, Z., 2016. Tribological properties and tribochemical analysis of nano-cerium oxide and sulfurized isobutene in titanium complex grease. Tribol. Int. 93, 332–346.

Shu, J., Harris, K., Munavirov, B., Westbroek, R., Leckner, J., Glavatskih, S., 2018. Tribology of polypropylene and Li-complex greases with ZDDP and MoDTC additives. Tribol. Int. 118, 189–195.

Singh, A.K., 2011. Castor oil-based lubricant reduces smoke emission in two-stroke engines. Ind. Crop. Prod. 33, 287–295.

Singh, J., Anand, G., Kumar, D., Tandon, N., 2016. Graphene based composite grease for elastohydrodynamic lubricated point contact. IOP Conf. Ser. Mater. Sci. Eng. 149, 12195.

Singh, J., Kumar, D., Tandon, N., 2018. Tribological and vibration studies on newly developed nano-composite greases under boundary lubrication regime. J. Tribol. 140, 32001.

Singh, J., Kumar, D., Tandon, N., 2017. Development of Nanocomposite Grease: Microstructure, Flow, and Tribological Studies. J. Tribol. 139, 52001.

Singh, T., 2020. Grease Production Survey Report for calendar year 2018, in: 22nd Lubricating Grease Conference, NLGI India-Chapter (2020). NLGI, Missouri.

Stachowiak, G.W., Batchelor, A.W. (Eds.), 2013. Engineering Tribology. Butterworth-Heinemann., Oxford, United Kingdom.

Sukirno, Fajar, R., Bismo, S., Nasikin, M., 2009. Biogrease Based on Palm Oil and Lithium Soap Thickener: Evaluation of Antiwear Property. World Appl. Sci. J. 6, 401–407.

Sukirno, Ludi, Rizqon, Bismo, Nasikin, 2010. Anti-wear properties of bio-grease from modified palm oil and calcium soap thickener. Agric. Eng. Int. CIGR J. 12, 64–69.

Sun, J., Du, S., 2019. Application of graphene derivatives and their nanocomposites in tribology and lubrication : a review. RSC Adv. 9, 40642–40661.

Syahir, A.Z., Zulkifli, N.W.M., Masjuki, H.H., Kalam, M.A., Alabdulkarem, A., Gulzar, M., Khuong, L.S., Harith, M.H., 2017. A review on bio-based lubricants and their applications. J. Clean. Prod. 168, 997–1016.

Talib, N., Nasir, R.M., Rahim, E.A., 2017. Tribological behaviour of modified jatropha oil by mixing hexagonal boron nitride nanoparticles as a bio-based lubricant for machining processes. J. Clean. Prod. 147, 360–378.

Tannous, J., Dassenoy, F., Lahouij, I., Le Mogne, T., Vacher, B., Bruhács, A., Tremel, W., 2011. Understanding the Tribochemical Mechanisms of IF-MoS_2 Nanoparticles Under Boundary Lubrication. Tribol. Lett. 41, 55–64.

Thottackkad, M.V., Perikinalil, R.K., Kumarapillai, P.N., 2012. Experimental Evaluation on the Tribological Properties of Coconut Oil by the Addition of CuO Nanoparticles. Int. J. Precis. Eng. Manuf. 13, 111–116.

Torbacke, M., Rudolphi, Å.K., Kassfeldt, E., 2014. Lubricants: introduction to properties and performance, First. ed. John Wiley & Sons, Ltd, Chichester, United Kingdom.

Totten, G.E. (Ed.), 1992. ASM Handbook, Volume 18: Friction, Lubrication, and Wear Technology. ASM International, Materials Park, Ohio.

Tzounis, L., Contreras-caceres, R., Schellkopf, L., Jehnichen, D., Fischer, D., Cai, C., Stamm, M., 2014. Controlled growth of Ag nanoparticles decorated onto the surface of SiO2 spheres : a nanohybrid system with combined SERS and catalytic properties. RSC Adv. 4, 17846–17855.

Vansant, E.F., Voort, P. Van Der, Vrancken, K.C., 1995. Characterization and Chemical Modification of the Silica Surface. Elsevier Science B. V., Amsterdam.

Vattikuti, S.V.P., Byon, C., 2015. Synthesis and Characterization of Molybdenum Disulfide Nanoflowers and Nanosheets: Nanotribology. J. Nanomater. Article ID, 1–

11.

Vengudusamy, B., Kuhn, M., Rankl, M., Spallek, R., 2016. Film Forming Behavior of Greases Under Starved and Fully Flooded EHL Conditions. Tribol. Trans. 59, 62–71.

Verma, D.K., Kumar, B., Kavita, Rastogi, R.B., 2018. Zinc Oxide- and Magnesium-Doped Zinc Oxide-Decorated Nanocomposites of Reduced Graphene Oxide as Friction and Wear Modifiers. ACS Appl. Mater. Interfaces 11, 2418–2430.

Wang, G., Yang, J., Park, J., Gou, X., Wang, B., Liu, H., Yao, J., 2008. Facile Synthesis and Characterization of Graphene Nanosheets. J. Phys. Chem. C 112, 8192–8195.

Wang, L., Wang, B., Wang, X., Liu, W., 2007. Tribological investigation of CaF_2 nanocrystals as grease additives. Tribol. Int. 40, 1179–1185.

Wang, L., Zhang, M., Wang, X., Liu, W., 2008. The preparation of CeF_3 nanocluster capped with oleic acid by extraction method and application to lithium grease. Mater. Res. Bull. 43, 2220–2227.

Wang, X., Shen, Z., Sang, T., Cheng, X., Li, M., Chen, L., Wang, Z., 2010. Preparation of spherical silica particles by Stöber process with high concentration of tetra-ethyl-orthosilicate. J. Colloid Interface Sci. 341, 23–29.

Wang, Z., Xia, Y., Liu, Z., Hu, T., 2010. Friction and wear behaviour of laser-textured surfaces under the lubrication of polyurea grease containing various additives. Proc. Inst. Mech. Eng. Part J J. Eng. Tribol. 225, 139–150.

Wu, P.R., Kong, Y.C., Ma, Z.S., Ge, T., Feng, Y.M., Liu, Z., Cheng, Z.L., 2018. Preparation and tribological properties of novel zinc borate/MoS_2 nanocomposites in grease. J. Alloys Compd. 740, 823–829.

Xiao, H., Dai, W., Kan, Y., Clearfield, A., Liang, H., 2015. Amine-intercalated α-zirconium phosphates as lubricant additives. Appl. Surf. Sci. 329, 384–389.

Xiao, H., Liu, S., 2017. 2D nanomaterials as lubricant additive: A review. Mater. Des. 135, 319–332.

Yamamoto, Y., Gondo, S., 2002. Frictional performance of lithium 12-hydroxystearate

greases with different soap fibre structures in sliding contacts. Lubr. Sci. 14, 349–362.

Yang, Y., Yamabe, T., Kim, B.-S., Kim, I.-S., Enomoto, Y., 2011. Lubricating Characteristic of Grease Composites with CNT Additive. Tribol. Online 6, 247–250.

Zachariah, Z., Nalam, P.C., Ravindra, A., Raju, A., Mohanlal, A., Wang, K., Castillo, R. V., Espinosa-Marzal, R.M., 2020. Correlation Between the Adsorption and the Nanotribological Performance of Fatty Acid-Based Organic Friction Modifers on Stainless Steel. Tribol. Lett. 68, 11.

Zainal, N.A., Zulkifli, N.W.M., Gulzar, M., Masjuki, H.H., 2018. A review on the chemistry, production, and technological potential of bio-based lubricants. Renew. Sustain. Energy Rev. 82, 80–102.

Zeng, X., Peng, Y., Yu, M., Lang, H., Cao, X.A., Zou, K., 2018. Dynamic Sliding Enhancement on Friction and Adhesion Dynamic Sliding Enhancement on Friction and Adhesion of Graphene , Graphene Oxide and Fluorinated Graphene. ACS Appl. Mater. Interfaces 10, 8214–8224.

Zhao, G., Zhao, Q., Li, W., Wang, X., Liu, W., 2013. Tribological properties of nano-calcium borate as lithium grease additive. Lubr. Sci. 26, 43–53.

Zhu, S., Huang, P., 2017. Influence mechanism of morphological parameters on tribological behaviors based on bearing ratio curve. Tribiology Int. 109, 10–18.

Appendix–A

Calculation of stoichiometric amount of 12–hydroxystearic acid and lithium hydroxide monohydrate required in the formulation of 250 gm grease sample

The molecular weight of thickener ingredients is listed in **Table A.1**.

Table A.1: Molecular weight of thickener ingredients

Name of thickener ingredients	Molecular weight (gm/mol)
12–hydroxystearic acid	300.53
Lithium hydroxide monohydrate	41.96
Lithium 12–hydroxystearate	306.40

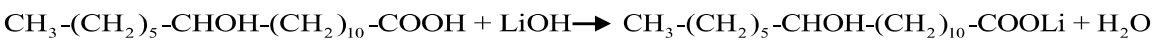

12–hydroxy stearic acid lithium hydroxide lithium 12–hydroxy stearate water

Moles of lithium 12–hydroxystearate in mixture $= \frac{\text{weight of compound}}{\text{molecular weight}}$

$= \frac{35 \text{ gm}}{306.4 \text{ gm/mol}} = 0.1142 \text{ mol}$

Weight of 12–hydroxystearic acid required = number of moles × molecular weight = 34.321 gm

Weight of lithium hydroxide monohydrate required = number of moles × molecular weight = 4.79 gm

Appendix–B

B.1 Calculation of Hertzian contact stress in case of four–ball tester

The four–ball tester form a point contact geometry and the area of contact will be circular. The radius of contact area is calculated as follows:

$$a = \left(\frac{3\, F_N\, R'}{E'} \right)^{\frac{1}{3}} \quad \text{(Stachowiak and Batchelor, 2013)} \quad \text{Eq (B1)}$$

Where,

a = radius of contact area or Hertzian radius [m];

F_N = Normal load [N];

R' = the reduced radius of curvature [m], i.e., $\frac{1}{R'} = \frac{1}{R_{x,A}} + \frac{1}{R_{x,B}} + \frac{1}{R_{y,A}} + \frac{1}{R_{y,B}}$,

where the subscripts ‘x’ and ‘y’ refer to x–direction and y–direction, respectively while subscripts ‘A’ and ‘B’ refer to body A and body B, respectively;

E' = the reduced Young’s modulus [Pa], i.e., $\frac{1}{E'} = \frac{1}{2}\left[\frac{1-\upsilon_A^2}{E_A} + \frac{1-\upsilon_B^2}{E_B} \right]$, where E_A and E_B are Young’s modulus, υ_A and υ_B are Poisson’s ratio of body A and B, respectively;

Maximum contact pressure (P_{max}) developed between contact point is calculated as follows:

$$P_{max} = \frac{3\, F_N}{2\pi\, a^2} \quad \text{Eq (B2)}$$

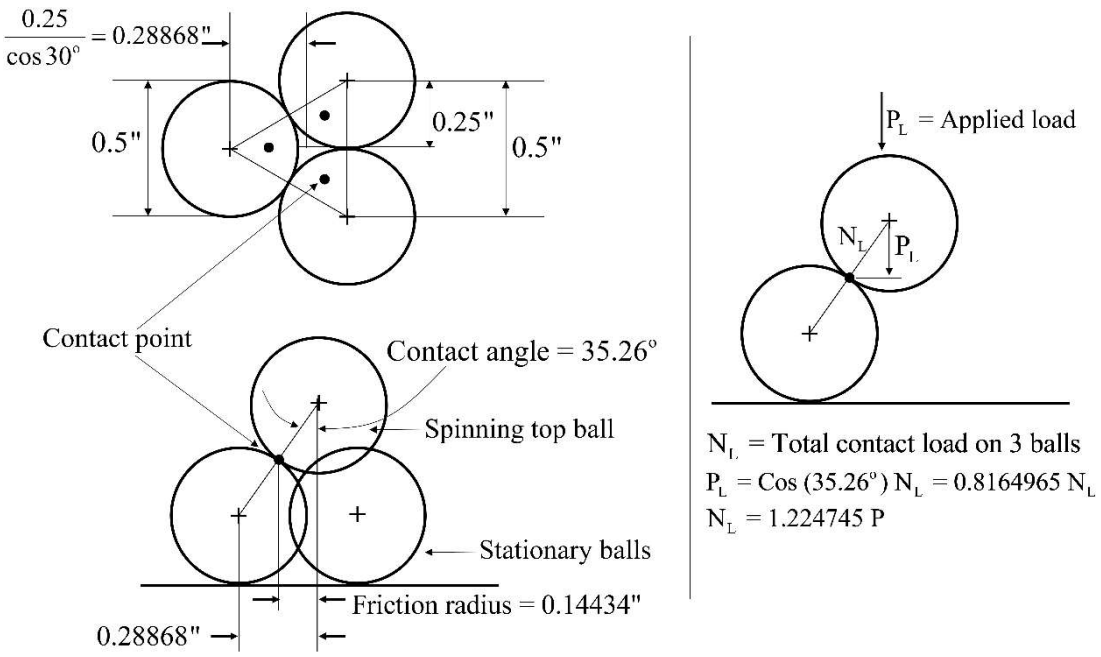

Figure B.1: Free body diagram of steel balls during tribo–test in four–ball tester

In case of AW test in four–ball tester, the diameter of steel balls (12.7 mm) is identical, and material properties are same. Therefore, $E_A = E_B = 210\ \text{GPa}$ and Poisson's ratio $\upsilon_A = \upsilon_B = 0.3$. **Figure B.1** shows free body diagram of steel balls during tribo–test in four–ball tester.

The reduced Young's modulus is calculated as follows,

$$\frac{1}{E'} = \frac{1}{2}\left[\frac{1-\upsilon_A^2}{E_A} + \frac{1-\upsilon_B^2}{E_B}\right]$$

$$\frac{1}{E'} = \frac{1}{2}\left[\frac{1-0.3^2}{210\times10^9} + \frac{1-0.3^2}{210\times10^9}\right]$$

$$E' = 2.3077\times10^{11}\ \text{Pa}$$

The diameter of steel balls is 12.7 mm.

The reduced radius of curvature,

$$\frac{1}{R'} = \frac{1}{R_{x,A}} + \frac{1}{R_{x,B}} + \frac{1}{R_{y,A}} + \frac{1}{R_{y,B}}$$

$$\frac{1}{R'} = \frac{1}{6.35\times10^{-3}} + \frac{1}{6.35\times10^{-3}} + \frac{1}{6.35\times10^{-3}} + \frac{1}{6.35\times10^{-3}}$$

$$R' = 1.5875\times10^{-3}\ \text{m}$$

In case of AW test with four–ball tester, the applied load (P_L) was 392 N.

Total normal load on 3 balls,

$$N_L = 1.224745\ P_L$$

Normal load on one ball,

$$F_N = \frac{N_L}{3} \Rightarrow \frac{1.224745\ P_L}{3}$$

$$F_N = \frac{1.224745\times392}{3}$$

$$F_N = 160.03\ \text{N}$$

The radius of contact area or Hertzian radius,

$$a = \left(\frac{3\ F_N\ R'}{E'}\right)^{\frac{1}{3}}$$

$$= \left(\frac{3\times160.03\times1.5875\times10^{-3}}{2.3077\times10^{11}}\right)^{\frac{1}{3}}$$

$$= 1.4892\times10^{-4}\ \text{m}$$

Maximum contact pressure or Hertzian contact stress

$$P_{max} = \frac{3\ F_N}{2\pi\ a^2}$$

$$= \frac{3\times160.03}{2\pi\ \left(1.4892\times10^{-4}\right)^2}$$

$$= 3444741785\ \text{Pa or } 3.44\ \text{GPa}$$

B.2 Calculation of Hertzian contact stress in case of SRV–5 test machine

The SRV–5 test machine forms a point contact geometry and the area of contact will be circular. The radius of contact area is calculated as follows:

$$a = \left(\frac{3\ F_N\ R'}{E'}\right)^{\frac{1}{3}} \qquad \text{Eq (B1)}$$

The reduced Young's modulus is calculated as follows,

$$\frac{1}{E'} = \frac{1}{2}\left[\frac{1-\upsilon_A^2}{E_A}+\frac{1-\upsilon_B^2}{E_B}\right]$$

$$\frac{1}{E'} = \frac{1}{2}\left[\frac{1-0.3^2}{210\times10^9}+\frac{1-0.3^2}{210\times10^9}\right]$$

$$E' = 2.3077\times10^{11}\ \text{Pa}$$

In SRV–5 test machine, 100Cr6 steel ball (ϕ = 10 mm) and disc (24×7.85mm) were used as the test specimen. Herein, the radii of the disc in $r_{x,\,disc}$, and $r_{y,}$ the disc is ∞

The reduced radius of curvature is,

$$\frac{1}{R'} = \frac{1}{R_{x,A}} + \frac{1}{R_{x,B}} + \frac{1}{R_{y,A}} + \frac{1}{R_{y,B}}$$

$$\frac{1}{R'} = \frac{1}{5\times10^{-3}} + \frac{1}{\infty} + \frac{1}{5\times10^{-3}} + \frac{1}{\infty}$$

$$R' = 2.5\times10^{-3}\ \text{m}$$

In case of AW test with SRV–5 test machine, the applied load (F_N) was 200 N.

The radius of contact area or Hertzian radius,

$$a = \left(\frac{3\ F_N\ R'}{E'}\right)^{\frac{1}{3}}$$

$$= \left(\frac{3\times200\times2.5\times10^{-3}}{2.3077\times10^{11}}\right)^{\frac{1}{3}}$$

$$= 1.8663\times10^{-4}\ \text{m}$$

Maximum contact pressure or Hertzian contact stress

$$P_{max} = \frac{3\ F_N}{2\pi\ a^2}$$

$$= \frac{3\times200}{2\pi\ \left(1.8663\times10^{-4}\right)^2}$$

$$= 274164250\ \text{Pa or } 2.74\ \text{GPa}$$

Appendix–C

C.1 Calculation of wear volume of worn surfaces of steel balls used in four–ball tester

The diameter of wear scar of each stationary balls was measured parallel and perpendicular to the sliding direction and geometric mean of these two diameters was reported as WSD of that particular ball is given by Eq (C1). Further, the average of three stationary balls was reported as mean scar diameter is given by Eq (C2).

Mean WSD, $$d_m = \sqrt{d_{\parallel}\, d_{\perp}} \quad \text{Eq (C1)}$$

Average WSD, $$d_{avg} = \frac{d_{m,1}+d_{m,2}+d_{m,3}}{3} \quad \text{Eq (C2)}$$

Hertzian diameter, $$d_o = 2\left(\frac{3\, F_N\, R'}{E'}\right)^{\frac{1}{3}} \quad \text{Eq (C3)}$$

Where,

d_o = diameter of contact area or Hertzian diameter [m];

$d_{m,1}$ = mean WSD of stationary steel ball 1 [m];

$d_{m,2}$ = mean WSD of stationary steel ball 2 [m];

$d_{m,3}$ = mean WSD of stationary steel ball 3 [m];

F_N = Normal load [N];

R' = the reduced radius of curvature [m], i.e., $\frac{1}{R'} = \frac{1}{R_{x,A}} + \frac{1}{R_{x,B}} + \frac{1}{R_{y,A}} + \frac{1}{R_{y,B}}$,

where the subscripts 'x' and 'y' refer to x–direction and y–direction, respectively while subscripts 'A' and 'B' refer to body A and body B, respectively;

E' = the reduced Young's modulus [Pa], i.e., $\frac{1}{E'} = \frac{1}{2}\left[\frac{1-\upsilon_A^2}{E_A} + \frac{1-\upsilon_B^2}{E_B}\right]$, where E_A and E_B are Young's modulus, υ_A and υ_B are Poisson's ratio of body A and B, respectively;

Wear volume, $$V = \frac{\pi d_0^4}{64R'}\left[\left(\frac{d_{avg}}{d_o}\right)^4 - \left(\frac{d_{avg}}{d_o}\right)\right] \qquad \text{Eq (C4)}$$

In case of AW test with four–ball tester, the diameter of steel balls (12.7 mm) is identical, and material properties are same. Therefore, $E_A = E_B = 210\ GPa$ and Poisson's ratio $\upsilon_A = \upsilon_B = 0.3$

The reduced Young's modulus,

$$\frac{1}{E'} = \frac{1}{2}\left[\frac{1-\upsilon_A^2}{E_A} + \frac{1-\upsilon_B^2}{E_B}\right] \qquad \text{Eq (C5)}$$

$$\frac{1}{E'} = \frac{1}{2}\left[\frac{1-0.3^2}{210\times10^9} + \frac{1-0.3^2}{210\times10^9}\right]$$

$$E' = 2.3077\times10^{11}\ Pa$$

The diameter of steel balls (d) is 12.7 mm.

The reduced radius of curvature,

$$\frac{1}{R'} = \frac{1}{R_{x,A}} + \frac{1}{R_{x,B}} + \frac{1}{R_{y,A}} + \frac{1}{R_{y,B}} \qquad \text{Eq (C6)}$$

$$\frac{1}{R'} = \frac{1}{6.35\times10^{-3}} + \frac{1}{6.35\times10^{-3}} + \frac{1}{6.35\times10^{-3}} + \frac{1}{6.35\times10^{-3}}$$

$$R' = 1.5875\times10^{-3}\ \text{m}$$

In case of AW test with four–ball tester, the applied load (P) was 392 N.

Total normal load on 3 balls,

$$N_L = 1.224745\ P_L \qquad \text{Eq (C7)}$$

Normal load on one ball,

$$F_N = \frac{N_L}{3} \Rightarrow \frac{1.224745\ P_L}{3} \qquad \text{Eq (C8)}$$

$$F_N = \frac{1.224745\times392}{3}$$

$$F_N = 160.03\ \text{N}$$

The diameter of contact area or Hertzian diameter,

$$d_o = 2\left(\frac{3\ F_N\ R'}{E'}\right)^{\frac{1}{3}}$$

$$= 2\times\left(\frac{3\times160.03\times1.5875\times10^{-3}}{2.3077\times10^{11}}\right)^{\frac{1}{3}}$$

$$= 2.978\times10^{-4}\ \text{m}$$

The mean WSD of three stationary steel balls lubricated with paraffin grease were 895.59 μm, 841.98 μm, and 824.74 μm. Therefore, the average WSD of three stationary steel balls

$$= \frac{896.59 + 841.98 + 824.74}{3}$$

$$= 854.43\ \mu m \text{ or } 8.544\times10^{-4}\ m$$

$$V = \frac{\pi\times\left(2.978\times10^{-4}\right)^4}{64\times1.5875\times10^{-3}}\left[\left(\frac{8.544\times10^{-4}}{2.978\times10^{-4}}\right)^4 - \left(\frac{8.544\times10^{-4}}{2.978\times10^{-4}}\right)\right]$$

$$V = 7.945\times10^{-11}\ m^3 \text{ or } 79.45\times10^{-4}\ mm^3$$

Similarly, the wear volume of each worn surfaces of steel balls lubricated with various grease samples were calculated.

C.1 Calculation of wear volume of worn surfaces of steel ball and disc used in SRV–5 test machine

The planimetric wear (W_q) of the disc was acquired across the wear track via profilometric measurements. The radius of the steel ball (R') after the test was measured by a profilometer and estimated the wear volume (W_V) of ball and disc using following equations (C9–C11):

$$W_{V,ball} = \frac{\pi\cdot d_{\perp}^2\cdot d_{\parallel}^2}{64}\left(\frac{1}{R} - \frac{1}{R'}\right) \quad \text{Eq (C9)}$$

$$W_{V,disc} = \frac{\pi\cdot d_{\perp}^2\cdot d_{\parallel}^2}{64}\frac{1}{R'} + \Delta x\cdot W_q \quad \text{Eq (C10)}$$

$$W_V = W_{V,ball} + W_{V,disc} \quad \text{Eq (C11)}$$

The wear coefficient (k) was computed by using the following equation:

$$k = \frac{W_V}{2 \cdot \Delta x \cdot n \cdot F_n} \qquad \text{Eq (C12)}$$

Herein, $W_{V,\,ball}$, and $W_{V,\,disc}$ represents wear volume of ball and disc, respectively. The $d_{\perp}$ and $d_{\parallel}$ express WSD perpendicular and parallel to the sliding direction, respectively. R and R' represent radius before and after the tribo–test, respectively. The Wq, Δx, and n are the planimetric wear (cross–section of wear scar from the profile), stroke length, and the number of cycles, respectively. **Figure C.1** explicitly illustrates the schematic diagram for the computation of wear volume.

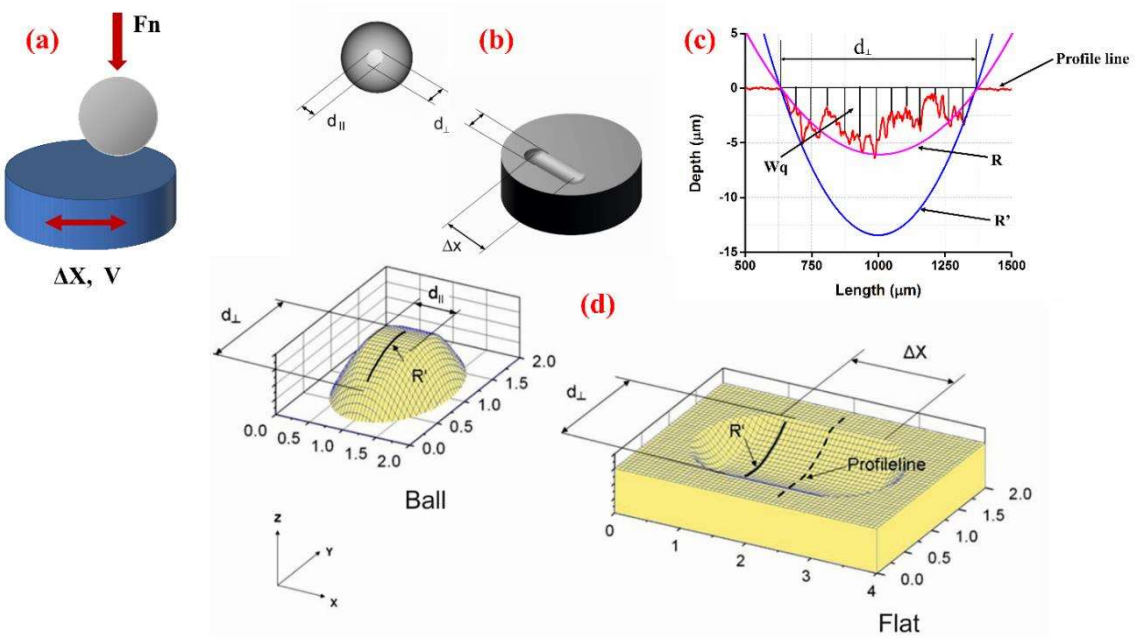

Figure C.1: Schematic view of (a) tribo–pair, (b) worn out specimens (c) profilometry of worn surfaces (d) 3D surface profile of worn track

Appendix–D

Film thickness calculation in case of four–ball tester

The minimum film thickness (h_{min}) was computed considering hard elastohydrodynamic lubrication (EHL) regime and calculated using Hamrock and Dowson equation (Stachowiak and Batchelor, 2013):

$$\frac{h_{min}}{R'} = 3.63\left(\frac{u\eta_o}{E'R'}\right)^{0.68}\left(\alpha E'\right)^{0.49}\left(\frac{F_N}{E'R'^2}\right)^{-0.073}\left(1-e^{-0.68k}\right) \qquad \text{Eq (D1)}$$

$$H = 3.63\left(U\right)^{0.68}\left(G\right)^{0.49}\left(W\right)^{-0.073}\left(1-e^{-0.68k}\right) \qquad \text{Eq (D2)}$$

The non–dimensional film parameter $H = \frac{h_{min}}{R'}$

The non–dimensional speed parameter $U = \left(\frac{u\eta_o}{E'R'}\right)$

The non–dimensional materials parameter $G = \left(\alpha E'\right)$

The non–dimensional load parameter $W = \left(\frac{F_N}{E'R'^2}\right)$

Where,

h_{min} = minimum film thickness [m];

u = the entertaining surface velocity [m/s], i.e., $u = \frac{u_A + u_B}{2}$, where u_A is velocity of body A and u_B is velocity of body B;

η_o = viscosity of base oil at atmospheric pressure [Pas];

E' = the reduced Young's modulus [Pa], i.e., $\frac{1}{E'} = \frac{1}{2}\left[\frac{1-\upsilon_A^2}{E_A}+\frac{1-\upsilon_B^2}{E_B}\right]$, where E_A and E_B are Young's modulus, υ_A and υ_B are Poisson's ratio of body A and B, respectively;

R' = the reduced radius of curvature [m], i.e., $\frac{1}{R'} = \frac{1}{R_{x,A}}+\frac{1}{R_{x,B}}+\frac{1}{R_{y,A}}+\frac{1}{R_{y,B}}$, where the subscripts 'x' and 'y' refer to x–direction and y–direction, respectively while subscripts 'A' and 'B' refer to body A and body B, respectively;

α = Pressure–viscosity coefficient [m^2/N];

F_N = normal load [N];

k = ellipticity parameter, i.e., $k = \frac{a}{b}$, where 'a' is semiaxis of the contact ellipse [m] (in the transverse direction), 'b' is the semiaxis of contact ellipse [m] (in the direction of motion)

The pressure–viscosity coefficient (α) was calculated by the empirical relation derived by Wooster, is given by equation (D3).

$$\alpha = (0.6 + 0.95\log_{10}\eta_o)\times 10^{-8} \qquad \text{Eq (D3)}$$

Where,

α = Pressure–viscosity coefficient [m^2/N]

η_o = Atmospheric viscosity [cP]

In case of AW test with four–ball tester, the diameter of steel balls (12.7 mm) is identical, and material properties are same. Therefore, $E_A = E_B = 210$ GPa and Poisson's ratio $\upsilon_A = \upsilon_B = 0.3$

The reduced Young's modulus,

$$\frac{1}{E'} = \frac{1}{2}\left[\frac{1-\upsilon_A^2}{E_A} + \frac{1-\upsilon_B^2}{E_B}\right] \qquad \text{Eq (D4)}$$

$$\frac{1}{E'} = \frac{1}{2}\left[\frac{1-0.3^2}{210\times10^9} + \frac{1-0.3^2}{210\times10^9}\right]$$

$$E' = 2.3077\times10^{11}\ \text{Pa}$$

The diameter of steel balls (D) is 12.7 mm.

The reduced radius of curvature,

$$\frac{1}{R'} = \frac{1}{R_{x,A}} + \frac{1}{R_{x,B}} + \frac{1}{R_{y,A}} + \frac{1}{R_{y,B}} \qquad \text{Eq (D5)}$$

$$\frac{1}{R'} = \frac{1}{6.35\times10^{-3}} + \frac{1}{6.35\times10^{-3}} + \frac{1}{6.35\times10^{-3}} + \frac{1}{6.35\times10^{-3}}$$

$$R' = 1.5875\times10^{-3}\ \text{m}$$

In case of AW test with four–ball tester, the applied load (P) was 392 N.

Total normal load on 3 balls,

$$N_L = 1.224745\ P_L \qquad \text{Eq (D6)}$$

Normal load on one ball,

$$F_N = \frac{N_L}{3} \Rightarrow \frac{1.224745\ P_L}{3} \qquad \text{Eq (D7)}$$

$$F_N = \frac{1.224745\times392}{3}$$

$$F_N = 160.03\ \text{N}$$

The entertaining surface 'A' velocity, $u_A = \dfrac{\pi\ D\ N}{60}$ Eq (D8)

$$= \frac{\pi\times12.7\times10^{-3}\times1200}{60}$$

$$= 0.7979 \text{ m/s}$$

Bottom balls were fixed, therefore $u_B = 0$

The entertaining surface velocity, $u = \frac{u_A + u_B}{2}$ Eq (D9)

$$= \frac{0.7979 + 0}{2}$$

$$= 0.3989 \text{ m/s}$$

The density (ρ) and kinematic viscosity (η_o) of different base oils are summarized in **Table 3.1**.

For paraffin oil, the density (ρ) and kinematic viscosity (η_k) of paraffin oil was 0.854 g/cm^3 (or 854 kg/m^3) and 81.17 mm^2/s (or 81.17×10^{-6} m^2/s), respectively.

Therefore, dynamic viscosity of paraffin oil, $\eta_o = \eta_k \times \rho$ Eq (D10)

$$= 81.17\times10^{-6}\times854$$

$$= 0.06931 \text{ Pas or } 69.31 \text{ cP}$$

The non–dimensional speed parameter $U = \left(\frac{u\eta_o}{E'R'}\right)$ Eq (D11)

$$= \left(\frac{0.3989\times0.0693}{2.307\times10^{-11}\times1.5875\times10^{-3}}\right)$$

$$= 7.548\times10^{-11}$$

The pressure–viscosity coefficient (α) was calculated by the empirical relation derived by Wooster, is given as follows:

$$\alpha = (0.6 + 0.95\log_{10}\eta_o)\times10^{-8}$$ Eq (D3)

$$= (0.6 + 0.95\times\log_{10}69.31)\times10^{-8}$$

$$= 2.348\times10^{-8}\ \text{m}^2/\text{N}$$

The non–dimensional materials parameter $G = \left(\alpha E^{'}\right)$ Eq (D12)

$$= 2.348\times10^{-8}\times2.307\times10^{11}$$

$$=5400.4$$

The non–dimensional load parameter $W = \left(\frac{F_N}{E^{'}R^{'2}}\right)$ Eq (D13)

$$= \frac{160.03}{2.307\times10^{11}\times\left(1.5875\times10^{-3}\right)^2}$$

$$= 2.752\times10^{-4}$$

Note: for point contact k = 1

Substitute the values of eq (D11), eq (D12), and eq (D13) in eq (D2)

$$H = 3.63\left(U\right)^{0.68}\left(G\right)^{0.49}\left(W\right)^{-0.073}\left(1\text{-}e^{-0.68k}\right)$$ Eq (D2)

$$H = 3.63\left(7.548\times10^{-11}\right)^{0.68}\left(5400.4\right)^{0.49}\left(2.752\times10^{-4}\right)^{-0.073}\left(1\text{-}e^{-0.68\times1}\right)$$

$$H = 3.63\times\left(1.309\times10^{-7}\right)\times\left(67.435\right)\times\left(1.819\right)\times\left(0.493\right)$$

$$\frac{h_{min}}{R^{'}} = 2.873\times10^{-5}$$

$$h_{min} = 2.873\times10^{-5}\times1.5875\times10^{-3}$$

$$h_{min} = 4.56\times10^{-8}\ \text{m or}\sim46\ \text{nm}$$

Further, the film thickness parameter (λ) was also assessed to determine the lubrication regime.

$$\lambda = \frac{h_{min}}{\sigma^{*}}$$ Eq (D14)

Where,

σ^* = composite surface roughness, i.e., $\sigma^* = \sqrt{\sigma_A^2 + \sigma_B^2}$, where, σ_A and σ_B are the surface roughness of body A and B, respectively.

$$\lambda = \frac{h_{min}}{\sqrt{\sigma_A^2 + \sigma_B^2}} \qquad \text{Eq (D15)}$$

The specifications of test specimens used in the tribo–test are listed in **Table 3.6**. Therefore, the surface roughness of ball A and ball B was 0.201 μm.

$$\lambda = \frac{4.56 \times 10^{-8}}{\sqrt{\left(0.201 \times 10^{-6}\right)^2 + \left(0.201 \times 10^{-6}\right)^2}}$$

$$\lambda = 0.1604$$

The λ value is less than one that signifies that tribo–pairs was operating under the boundary lubrication regime.

Similarly, for castor and coconut oil the h_{min} and λ was calculated and summarized in **Table D.1**.

Table D.1: Summary of calculated minimum film thickness and film thickness parameter for different base oils

Base oil	**Minimum film thickness (nm)**	**Film thickness parameter**
Paraffin	46	0.1604
Castor	115	0.4042
Coconut	21	0.0733

The $\lambda < 1$ for all base oils that signifies that tribo–pairs were operating under the boundary lubrication regime.

Appendix–E

Calculation of energy consumption due to friction in case of four–ball tester

In AW test conducted on four–ball tester, the frictional power loss was calculated as follows.

$$P_{loss} = T \bullet \omega \qquad \text{Eq (E1)}$$

Where,

P_{loss} = Frictional power loss [N.m.s^{-1}];

T = Frictional torque [N.m], i.e., $T = F_F \bullet r_F$;

ω = angular velocity [rad/s], i.e., $\omega = \frac{2\pi n}{60}$;

n = speed [rpm];

F_F = Frictional force [N], i.e., $F_F = \mu F_N$;

r_F = Friction radius [m];

μ = coefficient of friction;

F_N = Normal load [N];

Substituting all the values in eq. (E1), then frictional power loss

$$P_{loss} = 221 \times \mu \ [W] \qquad \text{Eq (E2)}$$

$$1\text{kWh} = 3.6\ \text{MJ} \qquad \text{Eq (E3)}$$

Appendix–F

Copyright permissions

SPRINGER NATURE

Thank you for your order!

Dear Mr. SOORAJ RAWAT,

Thank you for placing your order through Copyright Clearance Center's RightsLink® service.

Order Summary

Licensee:	Mr. SOORAJ S RAWAT
Order Date:	Jul 14, 2021
Order Number:	5107530580838
Publication:	Applied Nanoscience
Title:	Tribological performance of paraffin grease with silica nanoparticles as an additive
Type of Use:	Thesis/Dissertation
Order Total:	0.00 USD

View or print complete details of your order and the publisher's terms and conditions.

Sincerely,

Copyright Clearance Center

Tel: +1-855-239-3415 / +1-978-646-2777
customercare@copyright.com
https://myaccount.copyright.com

CCC RightsLink®

SPRINGER NATURE

Thank you for your order!

Dear Mr. SOORAJ RAWAT,

Thank you for placing your order through Copyright Clearance Center's RightsLink® service.

Order Summary

Licensee:	Mr. SOORAJ S RAWAT
Order Date:	Jul 14, 2021
Order Number:	5107550278486
Publication:	Journal of Materials Engineering and Performance
Title:	Effect of Graphene-Based Nanoadditives on the Tribological and Rheological Performance of Paraffin Grease
Type of Use:	Thesis/Dissertation
Order Total:	0.00 USD

View or print complete details of your order and the publisher's terms and conditions.

Sincerely,

Copyright Clearance Center

Tel: +1-855-239-3415 / +1-978-646-2777
customercare@copyright.com
https://myaccount.copyright.com

SPRINGER NATURE

Thank you for your order!

Dear Mr. SOORAJ RAWAT,

Thank you for placing your order through Copyright Clearance Center's RightsLink® service.

Order Summary

Licensee:	Mr. SOORAJ S RAWAT
Order Date:	Jul 14, 2021
Order Number:	5107550534978
Publication:	Springer eBook
Title:	Current and Future Trends in Grease Lubrication
Type of Use:	Thesis/Dissertation
Order Total:	0.00 USD

View or print complete details of your order and the publisher's terms and conditions.

Sincerely,

Copyright Clearance Center

Tel: +1-855-239-3415 / +1-978-646-2777
customercare@copyright.com
https://myaccount.copyright.com

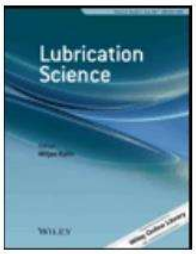

Thank you for your order!

Dear Mr. SOORAJ RAWAT,

Thank you for placing your order through Copyright Clearance Center's RightsLink® service.

Order Summary

Licensee:	Mr. SOORAJ S RAWAT
Order Date:	Jul 14, 2021
Order Number:	5107541317792
Publication:	Lubrication Science
Title:	Synergistic effect of binary systems of nanostructured MoS2/SiO2 and GO/SiO2 as additives to coconut oil-derived grease: Enhancement of physicochemical and lubrication properties
Type of Use:	Dissertation/Thesis
Order Total:	0.00 USD

View or print complete details of your order and the publisher's terms and conditions.

Sincerely,

Copyright Clearance Center

Tel: +1-855-239-3415 / +1-978-646-2777
customercare@copyright.com
https://myaccount.copyright.com

List of publications

Published manuscript

1. **Sooraj Singh Rawat**, A. P. Harsha, and Agarwal Pratik Deepak, Tribological Performance of Paraffin Grease with Silica Nanoparticles as an Additive, *Applied Nanoscience*, 2019, **9**(3), pp. 305–315.
   DOI: 10.1007/s13204–018–0911–9

2. **Sooraj Singh Rawat**, A. P. Harsha, Agarwal Pratik Deepak, Sangita Kumari, and Om P. Khatri, Pristine and Alkylated MoS_2 Nanosheets for Enhancement of Tribological Performance of Paraffin Grease under Boundary Lubrication Regime, *Journal of Tribology*, 2019, **141**(7), pp. 072102.
   DOI: 10.1115/1.4043606

3. **Sooraj Singh Rawat**, A. P. Harsha, Santanu Das, and Agarwal Pratik Deepak, Effect of CuO and ZnO Nano–Additive on the Tribological Performance of Paraffin Oil–Based Lithium Grease, *Tribology Transactions*, 2020, **63**(1), pp. 90–100.
   DOI: 10.1080/10402004.2019.1664684

4. **Sooraj Singh Rawat**, A. P. Harsha, Ajay Chouhan, and Om P. Khatri, Effect of Graphene–Based Nanoadditives on the Tribological and Rheological Performance of Paraffin Grease, *Journal of Materials Engineering and Performance*, 2020, **29**(4), pp. 2235–2247.
   DOI: 10.1007/s11665–020–04789–8

5. **Sooraj Singh Rawat**, A. P. Harsha, Om P. Khatri, and Rolf Wäsche, Pristine, Reduced, and Alkylated Graphene Oxide as Additives to Paraffin Grease for Enhancement of Tribological Properties, *Journal of Tribology*, 2021, **143**(2), pp. 021903.
   DOI: 10.1115/1.4047952

6. **Sooraj Singh Rawat**, A. P. Harsha, and Om P. Khatri, Synergistic Effect of Binary Systems of Nanostructured MoS_2/SiO_2 and GO/SiO_2 as Additives to Coconut Oil–Derived Grease: Enhancement of Physicochemical and Lubrication Properties, *Lubrication Science*, 2021, **33**(5), pp 290–307.
   DOI: 10.1002/ls.1554

Book Chapters

1. **Sooraj Singh Rawat**, and A. P. Harsha, Current and Future Trends in Grease Lubrication, *Automotive Tribology*, 2020, Springer, Singapore, pp. 147–182.

2. **Sooraj Singh Rawat**, and A. P. Harsha, Exploration of bio–greases for tribological applications**,** *Progress in Lubrication and Nano- and Biotribology Tribology, Lubrication, and Surface Engineering: Research and Applications*, 2021, CRC press, Taylor & Francis Group. pp. 75–101

3. **Sooraj Singh Rawat**, and A. P. Harsha, Recent progress in vegetable oil–based lubricants for tribological applications, *Tribology and Sustainability*, 2021, CRC press, Taylor & Francis Group, pp. 115–142.

Conferences/symposiums

1. Participated in National Tribology Conference (NTC–2016), December 8–10, 2016, Department of Mechanical Engineering, IIT (BHU), Varanasi, Uttar Pradesh, India.

2. **Sooraj Singh Rawat**, Agarwal Pratik Deepak, A. P. Harsha, and O. P. Khatri, Evaluation of tribological behavior of paraffin oil–based lithium greases with MoS_2 nanosheets as nano–additive, presented in 9th International Conference on Industrial Tribology (ICIT), December 6–9, 2017, Vedic village, Rajarhat, Kolkata, West Bengal, India. (**Oral presentation**)

3. **Sooraj Singh Rawat**, A. P. Harsha, O. P. Khatri, Evaluation of tribological behavior of paraffin oil–based lithium greases with graphene oxide and reduced graphene oxide nano–sheets as nano–additive, presented in TriboIndia–2018 an International Conference on Tribology, December 13–15, 2018, Veermata Jijabai Technical Institute, Mumbai, Maharashtra, India. (**Oral presentation**) (***Received second best paper award***)

4. **Sooraj Singh Rawat**, A. P. Harsha, Evaluation of the tribological behavior of paraffin oil–based lithium grease with CuO nano–additive, presented a poster in 3rd National Symposium on Shaping the Energy Future: Challenges and Opportunities (SEFCO–2019), May 10–11, 2019, CSIR Indian Institute of Petroleum, Dehradun, Uttarakhand, India. (**Poster presentation**)

5. **Sooraj Singh Rawat**, A. P. Harsha, Santanu Das, Evaluation of the tribological behavior of paraffin oil–based lithium grease with ZnO nano–additive, presented in IndiaTrib–2019 an International Conference on Industrial Tribology, December 1–4, 2019, Indian Institute of Science, Bangalore, Karnataka, India. (**Oral and poster presentation**)

6. **Sooraj Singh Rawat**, A. P. Harsha and O. P. Khatri, Synthesis, Characterization, and Tribological Evaluation of Reduced Graphene Oxide Added Grease through SRV–5, presented in 22nd Lubricating grease conference on Latest Trends in Grease Industry (NLGI India Chapter), February 1–3, 2020, Marriott Hotel Indore, Madhya Pradesh, India. (**Oral presentation**)

7. **Sooraj Singh Rawat** and A. P. Harsha, Exploration of tribological performance of coconut oil–based lithium greases, presented in International Tribology Research Symposium (ITRS – 2020) on Impact of Tribology on Society, November 5–7, 2020, SRM Institute of Science and Technology, Kattankulathur, Tamil Nadu, Shri Mata Vaishno Devi University, J&K, and Centre for Advanced Studies, AKTU, Lucknow, India. (**Oral presentation**)

8. **Sooraj Singh Rawat**, A. P. Harsha, Om P. Khatri, Evaluation of tribological performance of coconut oil–based grease with hybrid MoS_2/SiO_2 additives under boundary lubrication regime, presented paper in TriboIndia 2020 an International Virtual Conference on Tribology, December 10–12, 2020, by SRM Institute of Science and Technology, Kattankulathur, Tamil Nadu, India. (**Oral presentation**)

Response sheet for the examiner's comment

Comment No.	Questions	Reply to the comments	Remarks
1	What is meant by affinity?	The meaning of affinity is attraction. The vegetable oils have a great appeal towards metal surfaces to form a protective layer. It is a characteristic property of vegetable oils.	It has already been mentioned in the thesis. Therefore, no changes are required in the revised thesis.
2	The thesis uses to many acronyms to the extent that a reader not working in the area would find it difficult to read the thesis. I suggest that the acronyms be expanded the first time it is used in a given chapter.	As per the examiner's suggestion, the acronyms are expanded at the beginning of every chapter.	Changes have been made in Page no. 8, 56, 75, 98, 101, 110, 111, 128, 134, 137, 138, 141, 142, 146, 153, 155, 157, 163, and 174 of the revised thesis.
3	The moisture content is known to affect the tribological properties of MoS_2. Any specific precautions/ measurements done to take care of it during synthesizing and in subsequent storage of greases.	Yes, the moisture content affects the tribological properties of MoS_2. The MoS_2 nanosheets were prepared by hydrothermal technique. In the final step of the synthesis, the MoS_2 nanosheets were separated by filtration and dried in a conventional hot air oven at 90^0C to remove the moisture. Further, the nanomaterials and grease samples were stored in a desiccator to prevent the	The standard protocols were used and therefore no changes are required in the revised thesis.

		absorption of moisture. Therefore, appropriate care was taken while testing.	
4a	Hertzian contact radius, *a*, has a in the denominator. Please check. Provide the references for these equations. Using a specific equation like sphere (From see KL Johnson book) would be better than the general equation for bodies of arbitrary geometries.	The equation for Hertzian contact radius, '*a*', is correct. The equation was taken from the Engineering Tribology book edited by G.W. Stachowiak and A. W. Batchelor. The difference (KL Johnson book and GW Stachowiak book) observed in the equation mentioned above is due to a change in the reduced Young's modulus equation.	The reference for the Hertzian contact radius equation is included in the revised thesis (page no. 197).
4b	The resolved normal load, N, can never be greater than applied load P. The front view of the three views (bottom left in Figure B.1) doesn't seem to be correct. Please check the angle 35.26^{o}. From figure, it comes out to be a tan (0.28868/0.5)	The resolved normal load was calculated according to ASTM D5183 standard. The front view of the three views (bottom left in Figure B.1) is corrected and revised. The calculation for angle is verified and found to be correct.	Figure B.1 is corrected, and a modified figure is included in the revised thesis (page no. 198).
4c	The contact pressure obtained is too high. The hardness of the steel used would be approximately 0.8 to 1 GPa. The mean pressure used in practice would be much	The antiwear test was conducted according to ASTM D2266, and the contact pressure developed in the case of a four-ball tester was found to be 3.4 GPa, which is significantly higher than the hardness of steel. However, the grease was applied between the tribo-surfaces and thus formed a few nanometers thick lubricating film, which has separated the tribo-pairs and shares the contact	The test has been conducted as per ASTM standards. Therefore, no change is required in the thesis.

	below that to avoid plastic deformation. Please verify the calculations.	pressure. The pressures encountered in these contacts can be so high, and the rate of pressure rise so rapid that the lubricant behaves like a solid rather than a liquid. The load-bearing capacity of the grease is always tested at high contact pressure.	
4d	What is the radius $R_{Y,A}$ (6.35mm) (p195)?	The value of radius $R_{Y,A}$ is 5 mm. It is a typographical error.	The value of radius $R_{Y,A}$ is corrected in the revised thesis (page no. 201).
4e	Energy consumed will be more than what is calculated. Generally, there will be a viscosity component added along with friction component for lubricated contacts. Probably it is assumed that it would be negligible. Please, state that. It may not be negligible for greases but depends on how much greases was used?	The lube base oil offers a low shear strength lubricating film of a few nanometers thick. Therefore, the thickness of tribo-film in a few nanometers was found in the grease-lubricated condition and had low shear strength. Therefore, viscosity does not play any significant role.	No changes are required in the revised thesis.
5a	How much grease was applied at the contact, and how the constant supply was ensured?	The ball pot was filled with the grease sample and levelled off up to the top surface of the locknut. Approximately 12 to 15g quantity of grease was used. The interacting surfaces of balls are completely immersed in the grease. The temperature was maintained at 75^0C throughout the test run.	No changes are required in the revised thesis. The explanation is already been given in the thesis.

5b	What are the applied loads for the SEM images of the wear scars shown?	The antiwear test was conducted in a four-ball tester at 392 N and whereas in the SRV-5 test machine at 200 N. After completion of the test, the morphological features of the worn scars were captured in SEM.	The applied load is included in Figure the captions - 4.11, 4.12, 4.13, 4.14, 4.19, 4.20, 4.21, 4.22, 4.23, 4.24, 4.25, 4.26, 4.27, 4.28, 4.29, 4.30, 5.3, 5.4, 5.5, 5.6, 5.7, 5.8, 5.9, 5.10, 5.11, 5.12, 6.5, 6.6, 6.7, and 6.10 in the revised thesis.
5c	How long were the experiments carried out before examining the wear scars?	The experiments were conducted for 60 minutes on a four-ball tester and 120 minutes on an SRV-5 test machine.	The test duration is included in the Figure caption 4.11, 4.12, 4.13, 4.14, 4.19, 4.20, 4.21, 4.22, 4.23, 4.24, 4.25, 4.26, 4.27, 4.28, 4.29, 4.30, 5.3, 5.4, 5.5, 5.6, 5.7, 5.8, 5.9, 5.10, 5.11, 5.12, 6.5, 6.6, 6.7, and 6.10 in the revised thesis. The applied load and test duration were included in the Figure caption 4.11, 4.12, 4.13, 4.14, 4.19,

			4.20, 4.21, 4.22, 4.23, 4.24, 4.25, 4.26, 4.27, 4.28, 4.29, 4.30, 5.3, 5.4, 5.5, 5.6, 5.7, 5.8, 5.9, 5.10, 5.11, 5.12, 6.5, 6.6, 6.7, and 6.10 of the revised thesis.
5d	What are the operating parameters (at least the important ones) various characterization instruments used?	The operating parameters of various characterization instruments are included in the revised thesis.	Parameters are included in the following characterization instruments TEM (page no. 67) Grease microstructure SEM (page no. 76) SPM (page no. 82)
5e	Any background subtraction employed for the spectra reported?	No, there is no background subtraction employed for the reported spectra	No change is made in the revised thesis.

5f	The reported scatter bar is obtained from how many experiments. Is it indicating standard deviation or max-min.	Each experiment was repeated thrice and the average value of these results was reported. The scatter bar indicates the standard deviation.	No changes are required in the revised thesis. The explanation is already been given in the thesis.
6	The Mo-S stretching is indicated in figure 4.2 at 510 cm^{-1} instead of 472 mentioned in the text.	The infrared vibrations of MoS_2 show Mo–S stretching in the range between 450 to 650 cm^{-1} (Ref A,B). The vibrational peak at 510 cm^{-1} affirmed the formation of MoS_2 nanosheets. Ref A: Zheng G, Wu C, Wang J, Mo S, Wang Y, Zou Z, Zhou B, Long F. Facile synthesis of few-layer MoS_2 in MgAl-LDH layers for enhanced visible-light photocatalytic activity. RSC advances. 2019; 9(42): 24280-90 Ref B: Gao D, Si M, Li J, Zhang J, Zhang Z, Yang Z, Xue D. Ferromagnetism in freestanding MoS_2 nanosheets. Nanoscale research letters. 2013; 8(1): 1-8.	The value of Mo–S stretching is corrected in the revised thesis.
7	It is better to plot Figure 4.17 with log scale in y-axis, it gives an impression that viscosity is zero at higher strains	As per the examiner's suggestion, the Y-axis of Figure 4.17 is plotted in log scale.	Figure 4.17 is changed in the revised thesis (page no. 106)
8	It is surprising to see such clear abrasive tracks in all the experiments. Does the wear tracks look similar when only base	A typical feature of furrows in the direction of sliding is visible. The abrasion played a primary role in this event. If the tribo-pairs were tested under a boundary lubrication regime, the wear tracks	No changes are required in the revised thesis. The

	oil (complete immersion condition) is used instead of grease?	on the specimens were similar to the base oil used instead of grease.	explanation is already been given in the thesis.
9	Other than the XPS results for coconut oil, I don't see any significant proof of tribolayer. If it exists, it is too thin. Am I correct?	The XPS analysis confirms the formation of tribo-chemical thin film on the worn surfaces. Due to the limited availability of the XPS facility, the other worn surfaces were not assessed by XPS. However, the traces of nanoadditives on the worn surfaces have been confirmed by EDS analysis, and elemental mapping confirms the formation of tribolayer. The same nanoadditives were blended with other grease samples and evaluated for tribo-performance under similar test conditions. The nanoadditives have formed a tribo-film on the worn surfaces.	No changes are required in the revised thesis. The explanation is already been given in the thesis.
10	Maybe, at lower contact pressure, the behaviour of could have been very different.	The applied load has a significant effect on the tribological performance of the lubricant. When the applied load is low which results in a decrease in contact pressure. At lower or higher contact pressure, the tribological performance of lubricant could be very different.	No changes are required in the revised thesis.
11	How does the wear track evolves as a function of time? Maybe for future work. Was the experiment carried out long enough to complete the running-in phase?	The wear track generated depends upon the applied load, contact pressure, material and geometrical properties of tribo-pairs, sliding speed, and test conditions. The experiments were conducted as per the ASTM standard protocols and did not assess the running-in phase. In a four-ball tester, it is challenging to	No changes are required in the revised thesis.

		capture wear scar diameter at regular intervals. This will be explored in future work.	
12	Please define Mean Wear Volume. It should be just wear volume, I think. The units used are confusing may be μm^3 would be better.	The wear scar developed on the steel balls was elliptical. The mean diameter was calculated as per Eq. C1. Further, the wear volume was calculated as per Eq C4. The test was repeated three times, and the average value was reported, termed mean wear volume. Many researchers have reported the units in mm^3. Therefore, the wear volume unit in mm^3 is correct.	No changes are required in the revised thesis. The explanation is already been given in the thesis.
13	High stick-slip events – high adhesion resulting in roughness, please reflect on this. There are no evidences, unless I missed something. Maybe it needs elaboration. None of SEM images shows adhesive wear. Craters are too less to be significant in most images.	Corrugated features support the severity of wear in the form of the high stick-slip events because of high adhesion–driven wear. It further corroborates the friction and wear results that paraffin grease could not form a good quality tribo–film. The several undulations in the friction profile of paraffin grease (**Figure 4.12**) confirmed the poor–quality thin film along with the possibility of intermittent contact between the steel balls. The local coalescence of asperities and then breaking adhesive junctions due to sliding removed the materials in the form of wear (**Figure 4.21b**). The adhesive wear features are also explicitly seen in the SEM image (**Figure 4.19b**).	No changes are required in the revised thesis. The explanation is already been given in the thesis.

14	The roughness profiles shown in figure 6.10 is misleading. Probably the profile taken along the grooves rather than across the grooves (almost y-axis in figure 6.10 d, e and f). It is important to mention this. Typically, the roughness that tribologist are interested is across the grooves. The bearing area curve should also be across the grooves.	The roughness profiles shown in figure 6.10 are taken across the grooves, and the bearing area curve was also measured across the grooves.	No changes are required in the revised thesis.
15	When the COF of coconut oil (or any base oil used in the study) is in itself low (~0.1) where is the need for the "synergistic effect of additives"? The nanospheres and sheets are too less in number that the probability of them being trapped between asperities is too low. These particles are suspended in the solution. The conventional mechanism of boundary lubrication is the formation and reformation of protective monolayer by the long chain molecules on the surface due to interactions based on surface energy. This is generally sufficient to	The nanomaterials as additives to lubricating oils and greases improve the tribological properties because of their inherent properties. However, the synergistic blending of two different nanomaterials in the lubricating medium can furnish superior tribological properties than individual nanomaterials. The application of a binary system of two different types of nanoparticles for the formulation of environmentally-friendly vegetable oil-based grease has not been explored to furnish superior tribological properties. The raw coconut grease showed COF at 0.084, which reduced by 3%, 10%, and 10% in the presence of MoS_2, GO, and SiO_2 nanomaterials, respectively. The binary combinations of MoS_2/SiO_2 and GO/SiO_2 in variable wt% ratio as nanoadditives to coconut grease exhibited lower COF than individual materials. The MoS_2/SiO_2 combination in 30:70 ratio and GO/SiO_2	No changes are required in the revised thesis. The explanation is already been given in the thesis.

	bring the COF down to 0.05-0.1. It may be worthwhile to reflect on this.	combination in 50:50 ratio decreased the COF by 20% and 19%, respectively. It could be attributed to the synergistic effect of spherical SiO_2 nanoparticles and the 2D lamellar sheets of MoS_2 and GO. Likewise, the MWV of steel balls lubricated with MoS_2/SiO_2 (30:70) and GO/SiO_2 (50:50)-blended coconut grease reduced to 37% and 25%, respectively. The coconut oil exhibit inherently low frictional properties; however, it lacks the antiwear characteristic, particularly under the boundary lubrication regime (Ref). Herein, the synergistic combination of two different types of materials enhanced the friction-reducing properties of coconut grease and decreased wear by furnishing the antiwear properties. Ref: Jayadas NH, Prabhakaran Nair K, G A. Tribological evaluation of coconut oil as an environment-friendly lubricant. *Tribol Int*. 2007;40(2):350-354.	